Inorganic Chemistry

ARTICLE

pubs.acs.org/IC

Spin Structure of Surface-Supported Single-Molecule Magnets from Isomorphous Replacement and X-ray Magnetic Circular Dichroism

Matteo Mannini,[†] Erik Tancini,[‡] Lorenzo Sorace,[†] Philippe Sainctavit,[§] Marie-Anne Arrio,[§] Yu Qian,[§] Edwige Otero,[∥] Daniele Chiappe,[⊥] Ludovica Margheriti,[†] Julio C. Cezar,[#] Roberta Sessoli,[†] and Andrea Cornia*[,‡]

[†]Department of Chemistry 'Ugo Schiff' and INSTM RU, University of Florence, 50019 Sesto Fiorentino, Italy

[‡]Department of Chemistry and INSTM RU, University of Modena and Reggio Emilia, 41100 Modena, Italy

[§]Institut de Minéralogie et de Physique des Milieux Condensés, CNRS UMR7590, Université Pierre et Marie Curie, 75252 Paris, France

[∥]Synchrotron Soleil, Saint Aubin, 91192 Gif sur Yvette, France

[⊥]Department of Physics, University of Genova and CNISM, 16146 Genova, Italy

[#]European Synchrotron Radiation Facility (ESRF), 38043 Grenoble, France

Supporting Information

ABSTRACT: Surface-supported arrays of Fe_4-type Single-Molecule Magnets retain a memory effect and are of current interest in the frame of molecule-based information storage and spintronics. To reveal the spin structure of $[Fe_4(L)_2(dpm)_6]$ (**1**) on Au, an isomorphous compound $[Fe_3Cr(L)_2(dpm)_6]$ was synthesized and structurally and magnetically characterized (H_3L is tripodal ligand 11-(acetylthio)-2,2-bis(hydroxymethyl)undecan-1-ol and Hdpm is dipivaloylmethane). The new complex contains a central Cr^{3+} ion and has a $S = 6$ ground state as opposed to $S = 5$ in **1**. Low-temperature X-ray Magnetic Circular Dichroism studies at Fe- and Cr-$L_{2,3}$ edges revealed that the antiparallel alignment between Fe and Cr spins is preserved on surfaces. Moreover, the different Fe-$L_{2,3}$ spectral features found in the homo- and heterometallic species disclose the opposing contribution of the central Fe^{3+} ion in the former compound, proving that its ferrimagnetic spin structure is retained on surfaces.

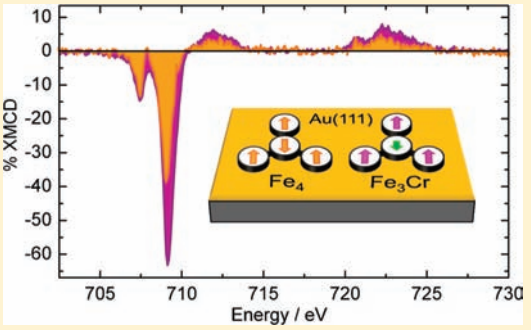

INTRODUCTION

The prospect of exploiting molecular spins to store and process information (molecular spintronics)[1] is driving fundamental investigations on the electronic structure and magnetism of open-shell molecular frameworks or molecular arrays at surfaces.[2] Single-Molecule Magnets (SMMs) in particular have been proposed as miniaturized memory units to be electrically written and read-out using an STM tip.[2,3] The electronic structure and functionality of these fragile metal complexes may however easily undergo profound alterations upon deposition, as found for the Mn_{12} family.[4] Special care must therefore be applied to rule out unwanted structural reorganization, fragmentation, or complete molecular disruption, which may take place during the grafting process.

We have recently shown that iron(III)-based SMMs of the Fe_4 family, $[Fe_4(L)_2(dpm)_6]$ (**1**) and $[Fe_4(L')_2(dpm)_6]$ (**2**), reinforced and functionalized using tripodal ligands H_3L = 11-(acetylthio)-2,2-bis(hydroxymethyl)undecan-1-ol[5a] and H_3L' = 7-(acetylthio)-2,2-bis(hydroxymethyl)heptan-1-ol,[5b] retain their structure and electronic properties on a gold surface (Hdpm = dipivaloylmethane). In fact, surface-supported complexes **1** and **2** exhibit a "memory effect", which is more pronounced in **2** because of its tendency to afford partially oriented layers.[5b] These magnetic investigations on molecules at surfaces, covering both static and dynamic properties, have largely relied on X-ray Magnetic Circular Dichroism (XMCD). XMCD is a spectroscopic technique derived from X-ray Absorption (XAS) and provides direct information on the magnetic polarization at specific elements.[6] Furthermore, when operated in the Total Electron Yield detection mode it becomes surface-sensitive and allows to probe the magnetism of monolayers or submonolayers,[4a,5,7] in a way not easily accessible to traditional magnetometry or magnetic resonance techniques.[7c,8]

Complexes of the Fe_4 series feature a *central* Fe^{3+} ion (Fe_c) with spin $s_i = 5/2$ antiferromagnetically coupled to three *peripheral* ones (Fe_p) to afford a ground state with total spin $S = 5$, as proved by magnetic measurements and electron paramagnetic resonance (EPR) spectroscopy.[5,9] This peculiar spin arrangement, in which uncompensation of antiparallel spins yields a large S value, is referred to as a *ferri*magnetic spin structure because of its

Received: October 29, 2010
Published: February 25, 2011

resemblance with the magnetic configuration of bulk ferrimagnets. The large magnetic moment in the ground state results in a XMCD signal at low temperature, which has the same intensity and fine structure in bulk samples and in monolayers.[5,10] The consistency of the observed XMCD response with a ferrimagnetic spin structure has found theoretical support from Ligand Field Multiplet (LFM) calculations,[10] but has never been experimentally verified.

We herein show that the XMCD response of **1** at Fe-$L_{2,3}$ edges is specific of its ground state spin configuration. To this aim, we have prepared a related compound, $[Fe_3Cr(L)_2(dpm)_6]$ (**3**), in which the central Fe^{3+} ion has been replaced by a Cr^{3+} ion (s_i = 3/2). According to previous work, such an isomorphous substitution can be carried out without metal scrambling, though residual Fe_4 species are found in the crystal lattice.[11] The resulting differences in the dichroic signal, detected both on bulk phase and on monolayer samples, disclose the field-opposing contribution of the central ion and demonstrate that **1** retains its ferrimagnetic spin structure on Au(111) surfaces.

EXPERIMENTAL SECTION

Synthesis. All operations were carried out with strict exclusion of moisture, unless otherwise stated. All chemicals were reagent grade and used as received, except for solvents, which were dried and distilled under nitrogen before use. Methanol was treated with $Mg(OMe)_2$ (prepared from Mg turnings, I_2, and MeOH) and distilled; diethylether and tetrahydrofuran (THF) were distilled from their blue Na/benzophenone solutions. 1,2-Dimethoxyethane (DME) and acetonitrile were treated with CaH_2 and distilled, acetonitrile being stored over 3A molecular sieves. The dimer $[Fe_2(OMe)_2(dpm)_4]$ (**4**) was prepared according to the procedure of Rossman et al.,[12a] modified as described in a previous publication.[9b] The compound $CrCl_3(THF)_3$ was prepared from $CrCl_3$ by prolonged Soxhlet extraction using anhydrous THF and zinc powder, as reported by Herwig and Zeiss.[12b] H_3L = 11-(acetylthio)-2,2-bis(hydroxymethyl)undecan-1-ol was synthesized as previously described.[9c] Sodium methoxide solution (3.08 M in methanol) was prepared by *careful* addition of sodium metal to anhydrous methanol under nitrogen. The Fe and Cr contents were measured by complexometric titration with EDTA (ca. 5×10^{-3} M), using back-titration with $Pb(NO_3)_2$ (ca. 5×10^{-3} M) and the technique of kinetic masking.[12c]

$[Fe_3Cr(L)_2(dpm)_6]$ (3). Compound **4** (0.5323 g, 0.5870 mmol) was suspended in a MeOH:Et_2O mixture (1:2 v/v, 50 mL) and stirred for 10 min. Solid $CrCl_3(THF)_3$ (0.1466 g, 0.3913 mmol) was then added in one portion, and the mixture stirred until complete dissolution of the solids to give a clear, dark-red solution (ca. 15 min). NaOMe (3.08 M in MeOH, 0.40 mL, 1.23 mmol) was introduced dropwise with vigorous stirring, and the mixture stirred for additional 30 min (a dark-red precipitate appeared). A MeOH:Et_2O mixture (1:4 v/v, 165 mL) was then added, and the reaction mixture was stirred for 1 h and left undisturbed overnight. The precipitated NaCl was filtered off using a G4 frit and washed extensively with Et_2O until colorless washings (ca. 50 mL). The liquid phase was evaporated at reduced pressure with gentle heating (30−40 °C) to give a brown powder (0.579 g). A portion of the solid (0.105 g, 0.0685 mmol Cr) and H_3L (0.0600 mg, 0.196 mmol, 2.7 equiv) were refluxed in DME (2 mL) for 4 h to give a dark brown solution. Slow evaporation of the solvent afforded a microcrystalline solid which was collected and washed extensively with methanol until colorless washings. The solid was suspended in the minimum amount of acetonitrile:DME (1:1) at 85 °C. Slow cooling of the clear solution afforded the desired product as red-black prisms that were collected by filtration, washed with acetonitrile and dried in vacuum (0.073 mg, 55% yield). Anal. Calcd. (%) for $Fe_{3.16}Cr_{0.84}C_{96}H_{168}O_{20}S_2$: C, 59.85; H, 8.79; S, 3.33; Cr, 2.27; Fe, 9.16. Found (average over two samples): C, 59.88; H, 8.80; S, 3.66; Cr, 2.33; Fe, 9.38 (Fe:Cr atom ratio 3.75:1). Alternative room-temperature routes were also tested, but they invariably afforded a lower Cr content.

X-ray Crystallography. The structure determination on **3** was carried out at 120(2) K using a 4-circle Bruker-Nonius X8APEX diffractometer, equipped with Mo-Kα radiation and a Kryo-Flex nitrogen flow cryostat. The structure was solved by direct methods using the SIR92 program.[13a] Full-matrix least-squares refinement on F_o^2 was performed using the SHELXL-97 program[13b] implemented in the WINGX suite.[13c] All non-hydrogen atoms were refined anisotropically, with the exception of the terminal portion of the alkyl chain, which was found disordered over three positions with 0.61, 0.21, and 0.18 occupancies and refined with restraints over geometrical and displacement parameters. In particular the $C-S-C(O)CH_3$ moiety was refined as a rigid group with the same geometry found in 1,2-ethanedithiol diacetate at 183 K.[13d] Hydrogen atoms were treated as riding contributors with isotropic displacement parameters. These were fixed to $U_H = pU_{iso}(C)$ where p = 1.2 for methine and methylene hydrogens, and p = 1.5 for methyl H atoms.

Magnetic Measurements. Direct Current (DC) magnetic data for a polycrystalline sample of **3** (8.40 mg), pressed in a pellet, were recorded on a Quantum Design MPMS SQUID magnetometer. Magnetic susceptibilities were measured in applied fields of 1 kOe from 1.9 to 35 K and 10 kOe from 35 to 300 K. Magnetization was also measured at 1.9, 2.5, and 4.5 K in fields up to 50 kOe. Data reduction was carried out using a molecular weight of 1926 and a diamagnetic contribution (estimated from Pascal's constants) of -1148×10^{-6} emu/mol. Alternating Current (AC) susceptibility in zero static field was measured in the frequency range 100−25000 Hz on a microcrystalline powder sample of **3** using an Oxford Instruments MAGLAB 2000 platform equipped with a home-built inductive coil probe.

W-band (ca. 94 GHz) EPR spectra were recorded on a polycrystalline powder sample of **3**, embedded in wax, using a Bruker Elexsys E600 CW spectrometer. Simulation of EPR spectra and spin-Hamiltonian calculations were carried out using a dedicated software, as described elsewhere.[9c,13e]

Monolayer Preparation. All the procedures were carried out in a portable glovebox inflated with nitrogen gas to avoid contamination of the surface or damaging of the molecular deposits. Polycrystalline Au, evaporated on a mica substrate (Agilent Inc.), was flame annealed with a hydrogen flame to achieve Au(111) reconstruction and cleaned with fresh ethanol (≥99.8% purity Aldrich) and dichloromethane (≥99.5% purity, Aldrich). The substrate was plunged in a 2 mM dichloromethane solution of **3** for 20 h so as to afford monolayer coverage. Overlayers of physisorbed molecules not directly grafted to the gold surface were removed by repeated washings with pure dichloromethane. A similar procedure already described elsewhere[5a] was used for the preparation of a monolayer of **1**. We expect that molecules form an homogeneous monolayer deposit, in analogy to our previous reports on **1**,[5a,14] with no preferential orientation on the surface. The substrate was mounted on the sample holder of the XMCD setup using a screwed copper mask. Bulk reference samples were thick films obtained by drop casting of 2 mM solutions of **1** or **3** in dichloromethane on a gold support.

XMCD Experiments. The XAS and XMCD experiments on bulk samples were carried out at the ID08 beamline of the European Synchrotron Radiation Facility (ESRF), Grenoble (France),[15a] and at the UE46-PGM beamline of BESSY II synchrotron, Helmholtz-Zentrum Berlin für Materialen und Energie (Germany).[15b] Monolayers were measured at the SIM-X11MA beamline of Swiss Light Source (SLS), Paul Scherrer Institut (PSI), Villigen (Switzerland).[15c] Drop cast and monolayer samples were inserted in a sample holder attached to the coldfinger of a ^{4}He cryostat working down to 7 K. Spectra were recorded at Fe- and Cr-$L_{2,3}$ edges (2p-3d transitions). All the measurements were carried out at very low X-rays photon flux, so as to avoid radiation

dx.doi.org/10.1021/ic102184n |*Inorg. Chem.* 2011, 50, 2911–2917

Table 1. Selected Interatomic Distances (Å) and Interbond Angles (deg) in 3, with Estimated Standard Deviation in Parentheses[a]

Cr1···Fe2	3.0100(10)	Cr1···Fe3	3.0119(6)	Fe2···Fe3	5.2250(8)
Fe3···Fe3′	5.1970(9)	Fe2···Cr1···Fe3	120.37(2)	Fe3···Cr1···Fe3′	119.25 (3)
Cr1−O1	1.961(2)	Cr1−O2	1.957(2)	Cr1−O3	1.956(2)
Fe2−O1	1.977(2)	Fe2−O4	2.000(2)	Fe2−O5	1.9943(19)
Fe3−O2′	1.980(2)	Fe3−O3	1.979(2)	Fe3−O6	2.002(2)
Fe3−O7	2.001(2)	Fe3−O8	2.003(3)	Fe3−O9	2.003(2)
O2−Cr1−O1	90.15(9)	O3−Cr1−O1	90.62(9)	O3−Cr1−O2	90.65(9)
O1′−Cr1−O1	80.70(12)	O2′−Cr1−O1	100.07(9)	O3′−Cr1−O1	166.16(9)
O2′−Cr1−O2	166.63(14)	O3′−Cr1−O2	80.72(9)	O3′−Cr1−O3	99.80(13)
O1′−Fe2−O1	79.89(12)	O4−Fe2−O1	93.50(9)	O5−Fe2−O1	96.92(9)
O5−Fe2−O4	86.28(9)	O5′−Fe2−O5	168.75(14)	O4′−Fe2−O1	172.82(9)
O5′−Fe2−O1	91.71(9)	O4′−Fe2−O4	93.23(14)	O5′−Fe2−O4	86.00(9)
O3−Fe3−O2′	79.60(9)	O3−Fe3−O7	169.96(11)	O2′−Fe3−O7	92.19(10)
O3−Fe3−O6	89.56(9)	O2′−Fe3−O6	97.94(10)	O7−Fe3−O6	85.84(10)
O3−Fe3−O9	97.48(9)	O2′−Fe3−O9	89.66(10)	O7−Fe3−O9	88.16(10)
O6−Fe3−O9	170.49(9)	O3−Fe3−O8	95.93(10)	O2′−Fe3−O8	172.89(10)
O7−Fe3−O8	92.79(11)	O6−Fe3−O8	87.49(10)	O9−Fe3−O8	85.43(10)
Cr1−O1−Fe2	99.71(10)	Cr1−O2−Fe3′	99.80(10)	Cr1−O3−Fe3	99.88(10)

[a] Primed atoms are related to unprimed ones by a 2-fold rotation along Cr1···Fe2.

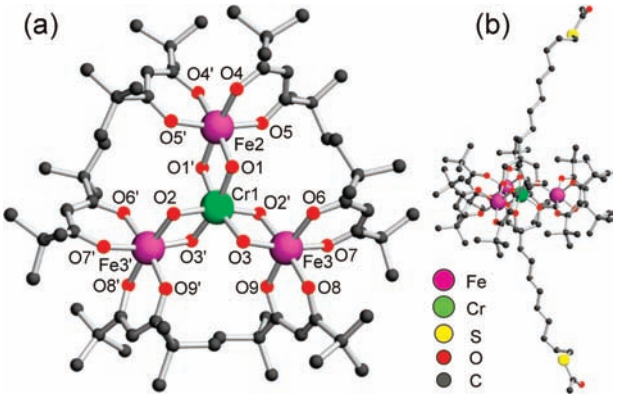

Figure 1. Core structure (a) and complete molecular structure (b) of **3** determined by X-ray diffraction at 120(2) K, omitting H atoms and disorder on alkyl chains. Primed atoms are related to unprimed ones by a 2-fold rotation around Cr1···Fe2.

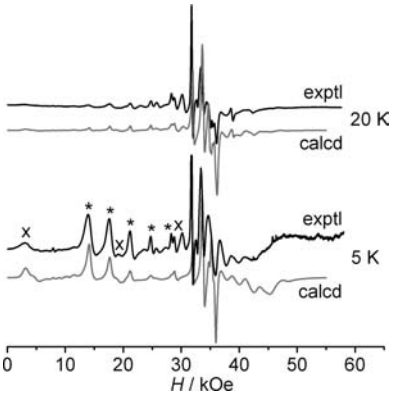

Figure 2. Experimental and simulated EPR spectra of **3** at 94.24 GHz. Asterisks and crosses mark the parallel type bands assigned to Cr-centered Fe_3Cr ($S = 6$) and Fe_4 species ($S = 5$), respectively.

damaging effects,[10] and in the Total Electron Yield (TEY) detection mode to achieve the required surface sensitivity.[15d] XMCD spectra were evaluated as $(\sigma^- - \sigma^+)$, where σ^- and σ^+ are the measured cross sections for right and left circularly polarized light, respectively (that is, for photon helicity vector antiparallel and parallel, respectively, to the applied magnetic field). To minimize systematic errors, each XMCD spectrum was obtained from eight measurements taken by switching the polarization and the field.[15e] In the experiments, we also checked the absence of any preferential orientation of molecules on the surface (no X-ray Natural Linear Dichroism) so that $(\sigma^+ + \sigma^-)/2$ was considered a good approximation to the isotropic spectrum in the electric dipole approximation. All reported XMCD contributions are normalized, that is, they are obtained by dividing the measured XMCD signal by the edge-jump of the isotropic absorption spectra at the energy of its maximum amplitude. Therefore, the XMCD spectra are proportional to the XMCD response *per metal atom*.

RESULTS AND DISCUSSION

Compound $[Fe_3Cr(L)_2(dpm)_6]$ (**3**) was synthesized by reacting $[Fe_2(OMe)_2(dpm)_4]$ with $CrCl_3(THF)_3$ and NaOMe in a Et_2O:MeOH mixture, removing the precipitated NaCl, evaporating the solvent completely, and refluxing the solid residue with excess H_3L in DME (eq 1). A final recrystallization from acetonitrile:DME afforded **3** as red-black prisms in 55% yield.

$$(3/2)[Fe_2(OMe)_2(dpm)_4] + CrCl_3(THF)_3 + 3NaOMe + 2H_3L \rightarrow [Fe_3Cr(L)_2(dpm)_6] + 3NaCl + 3THF + 6MeOH \quad (1)$$

Chemical analysis indicates that the Cr:Fe ratio (1:3.75) in the solid is lower than used in the synthesis (1:3). As described below, the location of the chromium(III) ions was clearly revealed by structural data, EPR spectra and magnetic measurements.

Single-crystal X-ray diffraction was used to determine the crystal and molecular structure of **3** (see Figure 1 and Supporting Information, Figure S1).[16] Selected structural parameters for **3** are gathered in Table 1. Although **1** and **3** are isomorphous, differences stand out clearly when examining the coordination geometry of the metal ions. While the average M−O distances for the peripheral ions in **1** and **3** are identical within experimental

dx.doi.org/10.1021/ic102184n |*Inorg. Chem.* 2011, 50, 2911–2917

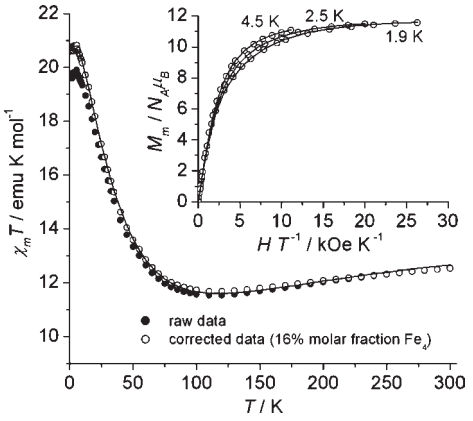

Figure 3. Raw and corrected DC magnetic data for **3**, with best fit calculated curves (solid lines). The main panel displays $\chi_m T$ vs T data, while the inset shows M_m vs H/T data recorded at three temperatures. For the sake of clarity, raw magnetization data are omitted.

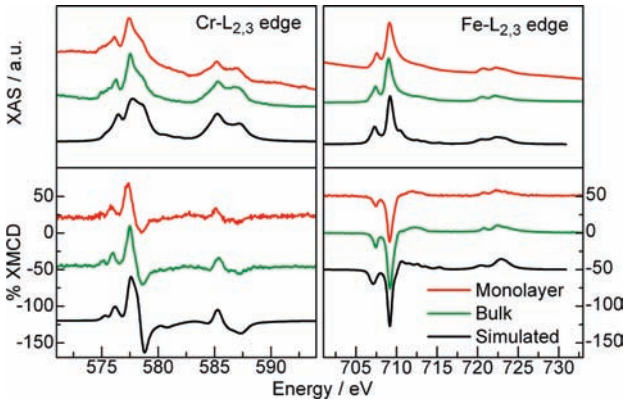

Figure 4. XAS and XMCD spectra obtained at 30 kOe and 7 K for monolayer and bulk samples of **3**, along with Ligand Field Multiplet simulations. XAS is presented in the isotropic form $(\sigma^- + \sigma^+)/2$; XMCD is evaluated as $(\sigma^- - \sigma^+)$ and is normalized with respect to the isotropic signal (see Experimental Section). A vertical offset has been applied to the spectra for a better presentation.

error (1.993(11) vs 1.991(13) Å), the central ion in **3** forms shorter bonds with the bridging O atoms of the tripod (1.958(3) vs 1.983(5) Å). In addition, the pitch of the helical structure, defined as the average dihedral angle between the M1(O)$_2$Fe2 and M1(O)$_2$Fe3 moieties (M = Fe, Cr) and the metal ion plane, is distinctly smaller in **3** (62.2° vs 67.3°).[9,11] These differences suggest that the central ion in **3** is smaller than in **1** by about 0.02 Å, as expected for a Cr-centered species.[17]

The EPR spectra of a polycrystalline sample of **3** were recorded at ν = 94.24 GHz in the temperature (T) range 5−20 K (Figure 2). Below the central field $H_0 = h\nu/(2\mu_B)$ = 33.66 kOe the spectrum at 5 K exhibits a pattern of almost equally spaced signals (marked with asterisks in Figure 2). Their intensity variation with field (H) and T is typical for parallel-type bands in a high-spin system with easy-axis anisotropy ($D < 0$).[18] From the position of the five visible lines, it can be inferred that six such transitions appear below H_0. This indicates that the ground state has total spin $S = 6$, which is the value expected for a Cr-centered Fe$_3$Cr species with antiferromagnetic Fe−Cr interactions. The line-to-line separation also provides $|D|$ about 0.16−0.17 cm^{-1}, while the broadening of perpendicular bands at $H > H_0$ is suggestive of a very weak rhombic anisotropy.[18] A further series of weaker signals, marked by crosses in Figure 2 and spanning a wider field range at $H < H_0$, is easily assigned to Fe$_4$ species on the basis of the line-to-line separation and of the observed temperature and field dependence.[9] If the compound is taken as a solid solution of Cr-centered Fe$_3$Cr and Fe$_4$, the observed Fe:Cr ratio implies the presence of 84% Fe$_3$Cr and 16% Fe$_4$. Notably, very similar results were obtained using a different tripodal ligand.[11] The given composition allowed an accurate reproduction of the spectra using the spin-Hamiltonian[9c,13e]

$$\hat{\mathbf{H}}_{EPR} = \mu_B \hat{\mathbf{S}}\cdot\mathbf{g}\cdot\hat{\mathbf{H}} + D[\hat{S}_z^2 - S(S+1)/3] + E(\hat{S}_x^2 - \hat{S}_y^2) + B_4^0\hat{\mathbf{O}}_4^0 \quad (2)$$

where $\hat{\mathbf{S}}$ is the total spin operator (with components $\hat{S}_x$, $\hat{S}_y$, and $\hat{S}_z$), $\hat{\mathbf{O}}_4^0$ is the fourth-order axial anisotropy operator, and the other symbols have their usual meaning. The best-fit parameter set was (for Fe$_3$Cr) $S = 6$, $D = -0.165(2)$ cm^{-1}, $E = 0.005(1)$ cm^{-1}, $B_4^0 = 0.0(1)\cdot10^{-5}$ cm^{-1}, $g_{x,y} = 1.990(2)$, $g_z = 2.000(2)$; (for Fe$_4$) $S = 5$, $D = -0.405(2)$ cm^{-1}, $E = 0.018(4)$ cm^{-1}, $B_4^0 = 1.5(2)\cdot10^{-5}$ cm^{-1}, $g_{x,y} = 1.995(2)$, $g_z = 2.005(2)$.

DC magnetic data of **3**, recorded in the form of low-field χ_m vs T and isothermal M_m vs H curves, are in accordance with the proposed composition and spin ground state. Low-field $\chi_m T$ vs T data, displayed in Figure 3, are typical for antiferromagnetic systems featuring a high-spin ground state.[11] After correction for the presence of 16% Fe$_4$, based on the known susceptibility values for **1**,[9a] the $\chi_m T$ value at low temperature is very close to the Curie constant for a $S = 6$ state with $g = 2.00$ (21 emu K mol^{-1}). Data at $T \geq 5$ K were accurately fitted using an isotropic Heisenberg *plus* Zeeman spin-Hamiltonian with nearest-neighbor ($J_{Fe\text{-}Cr}$) and next-nearest-neighbor ($J_{Fe\text{-}Fe}$) coupling constants (eq 3).

$$\hat{\mathbf{H}} = J_{Fe\text{-}Cr}\hat{\mathbf{s}}_1\cdot(\hat{\mathbf{s}}_2 + \hat{\mathbf{s}}_3 + \hat{\mathbf{s}}_{3'}) + J_{Fe\text{-}Fe}(\hat{\mathbf{s}}_2\cdot\hat{\mathbf{s}}_3 + \hat{\mathbf{s}}_3\cdot\hat{\mathbf{s}}_{3'} + \hat{\mathbf{s}}_{3'}\cdot\hat{\mathbf{s}}_2) + \mu_B g\hat{\mathbf{S}}\cdot\hat{\mathbf{H}} \quad (3)$$

(1 is the central Cr^{3+} ion, with spin $s_1 = 3/2$; 2, 3, and 3′ label the peripheral Fe^{3+} ions, each with spin $s_i = 5/2$). The best fit parameters were $J_{Fe\text{-}Cr} = 16.34(10)$ cm^{-1}, $J_{Fe\text{-}Fe} = 0.57(3)$ cm^{-1}, and $g = 1.9868(11)$). Isothermal M_m vs H data, also reported in Figure 3, were corrected as above and fitted using an axial zero-field splitting Hamiltonian (eq 4)[9c]

$$\hat{\mathbf{H}}_{zfs} = \mu_B g\hat{\mathbf{S}}\cdot\hat{\mathbf{H}} + D[\hat{S}_z^2 - S(S+1)/3] \quad (4)$$

with $S = 6$, $D = -0.154(3)$ cm^{-1}, and $g = 1.964(3)$.

On the basis of the D value determined by EPR, we obtain the expected anisotropy barrier as $U/k_B = |D/k_B|S^2 = 8.5(1)$ K, hence smaller than in **1** (ca. 16 K)[9a] but still large enough to induce the slow relaxation of the magnetization typical of SMMs. The frequency dependence of the real and imaginary components of AC susceptibility was measured in zero static field, in the frequency range ν = 100−25000 Hz and at temperatures down to 1.8 K (Supporting Information, Figure S2). The temperature dependence of the relaxation time follows Arrhenius law $\tau = \tau_0 \exp(U_{eff}/k_BT)$ with $\tau_0 = 1.5(4) \times 10^{-7}$ s and $U_{eff}/k_B = 8.1(5)$ K and is thus indicative of a thermally activated relaxation process (Supporting Information, Figure S3). The value of the effective barrier, U_{eff}/k_B, is in good agreement with the total splitting of the $S = 6$ multiplet in zero field ($U/k_B = 8.5(1)$ K).

dx.doi.org/10.1021/ic102184n |*Inorg. Chem.* 2011, 50, 2911–2917

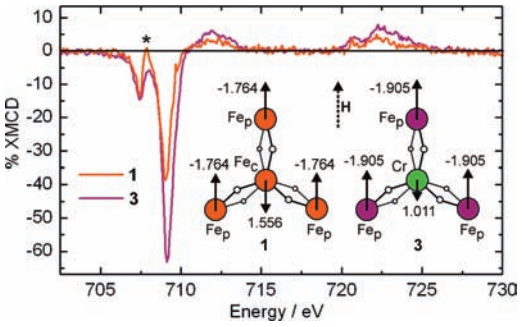

Figure 5. XMCD contribution at the Fe-$L_{2,3}$ edges (evaluated as a fraction of the isotropic signal) measured on monolayers of **1** and **3** at 30 kOe and 7 K. A schematic view of the metal core in **1** and **3** is also provided; numbers give the calculated spin component $s_z(i)/\hbar$ along the applied field **H** at each metal site; black arrows depict the corresponding magnetic moment, $-g\mu_B s_z(i)$; the asterisk marks the feature at 707.9 eV dicussed in the text.

A slower relaxation process is also visible which we attribute to the minority Fe_4 component.

All magnetic data coherently indicate that compound **3** has the same ferrimagnetic spin structure of **1**. However, it is an heterometallic system, and its central Cr^{3+} ion was exploited as an additional internal spectroscopic probe for combined XAS/XMCD studies at Fe-$L_{2,3}$ and Cr-$L_{2,3}$ edges. Monolayer deposits of **3** on Au(111) were assembled from dichloromethane solution, as described for **1** and **2**.[5,14] Their XAS and XMCD spectra at 30 kOe and 7 K are similar to those recorded on bulk references, obtained by drop casting (Figure 4 and Supporting Information, Figure S4). In both cases, the XMCD signal reaches its maximum amplitude at 709.1 eV (Fe-L_3 edge) and 577.5 eV (Cr-L_3 edge) and displays the same fine structure, indicating a similar electronic structure for the monolayer and for the bulk phase (small intensity differences may arise from the relevant baseline signal of the gold surface in the monolayer deposit, which influences the normalization procedure). Moreover, whereas the features observed at Fe-$L_{2,3}$ edges are characteristic for field-polarized high-spin Fe^{3+} ions,[19] the signal at Cr-$L_{2,3}$ edges is of opposite sign than for an isolated Cr^{3+} ion. This suggests that the magnetic polarization of Cr opposes the applied field and that Fe and Cr spins are antiparallel in both bulk and monolayer samples. To check the consistency between the measured XAS/XMCD spectra and the electronic structure of **3**, as determined by EPR and magnetic investigations, we have carried out Ligand Field Multiplet (LFM) calculations (see Supporting Information for details). The simulated spectra, reported in Figure 4 and Supporting Information, Figure S5, compare well with the observed ones in both intensity and fine structure and lend quantitative support to the above analysis.

Since the Fe^{3+} ions in **1** and **3** have very similar coordination environments, a meaningful comparison can be made between the XMCD features shown by monolayers of the two compounds at the Fe-$L_{2,3}$ edges (Figure 5). At the same T and H values, the amplitude of the dichroic component at 709 eV increases from 39% to 63% when replacing the central Fe^{3+} with Cr^{3+} (a similar trend was observed on bulk samples, with percentages of 40% and 76%; see Supporting Information, Figure S4). If the contribution of Fe_4 complexes is subtracted, assuming that their molar fraction in the monolayer is the same as in the bulk, the XMCD signal indeed reaches 70%. We checked whether such a large increase in the magnetic polarization at iron sites can be ascribed to the suppression of the opposing contribution of the central Fe^{3+} so as to provide direct proof of the ferrimagnetic ground state spin structure in **1**. To this aim, we have calculated the spin component in the applied field direction (z) at each metal site ($s_z(i)$), using the solid-state J-values with $g = 2.000$, $H =$ 30 kOe, T = 7 K and disregarding magnetic anisotropy for simplicity. Notice that the first-excited exchange multiplets in **1** and **3** lie 37.5 and 20.2 cm^{-1}, respectively, above the ground state, so that their thermal population is negligible in the temperature range of interest. A rigid-spin behavior is then followed and the $s_z(i)$ values are simply proportional to the molecular S_z as given by the appropriate Brillouin function.[20] The numeric values of $s_z(i)$ calculated at iron sites of **1** and **3** are presented in the inset of Figure 5 and in Supporting Information, Table S1. The average spin component *per iron site* is then given by $[3s_z(Fe_p) + s_z(Fe_c)]/4 = -0.934\hbar$ in **1** and as $s_z(Fe_p) = -1.905\hbar$ in **3**. Assuming the XMCD signal to be the same for Fe_p and Fe_c and proportional to the local magnetic moment, the normalized XMCD signal is expected to undergo an approximately 2-fold increase on passing from **1** to **3**, as experimentally observed.

A deeper comparison between the XMCD signals of **1** and **3** at the Fe-L_3 edge reveals another relevant difference. At an energy of about 707.9 eV (marked by an asterisk in Figure 5) the dichroic signal is negative in **3** but close to zero in **1**. The former behavior is typical for octahedral high-spin FeO_6 complexes.[19] Since the coordination geometry of Fe_p ions in the two compounds is virtually identical, the feature observed in **1** at 707.9 eV may reflect differences in the energy dependence of the XMCD contribution for Fe_p and Fe_c, because of their inequivalent coordination spheres.

CONCLUSIONS

XMCD is becoming of widespread use to reveal the electronic structure of magnetic molecules at surfaces. Many studies focused on simple metal-ion complexes, such as metal-porphirinato[7a,b] and metal bis(phthalocyaninato) species,[7c] whose crystal field parameters and magnetic properties were found to be robust upon adsorption on a metal substrate. With their complex and fragile architectures, polynuclear SMMs pose new challenges in XMCD analysis. We have shown here that the XMCD spectrum of a tetrairon(III) SMM at Fe-$L_{2,3}$ edges contains fingerprints of its spin structure. Upon isomorphous replacement of the central iron(III) with a chromium(III) ion, the intensity and shape of the signal change significantly, in agreement with the field-opposing magnetic contribution of the central ion. Substitution has the same effect in both bulk and monolayer samples, confirming that Fe_4 complexes have a ferrimagnetic spin structure on surfaces. It also follows that, although much weaker than crystal field splittings, superexchange interactions between metal ions can maintain the same sign in bulk samples and on surfaces.[7d] The herein-demonstrated specificity of Fe_4 XMCD response is now expected to have a far-reaching usefulness in the development of more demanding deposition methods, including thermal evaporation in high vacuum and deposition on more reactive substrates, like ferromagnetic metals.

ASSOCIATED CONTENT

Supporting Information. Additional crystallographic diagrams for **3** (showing thermal ellipsoids), crystallographic

dx.doi.org/10.1021/ic102184n |*Inorg. Chem.* 2011, 50, 2911–2917

data in CIF format, details of AC magnetic characterization, of XAS and XMCD data treatment and of LFM calculations. This material is available free of charge via the Internet at http://pubs.acs.org.

AUTHOR INFORMATION

Corresponding Author
*E-mail: acornia@unimore.it. Phone: +39-059-2055032. Fax: +39-059-373543.

ACKNOWLEDGMENT

We thank F. Scheurer, J. P. Kappler, B. Muller, P. Imperia, F. Nolting, and N. Brookes for their contribution to the development of the XMCD setup employed in this work. The research was funded by the European Community (ELISA grant agreement no. 226716, MolSpinQIP FP7-ICT-2007-C-211284 and ERANET "NanoSci-ERA: Nanoscience in European Research Area" projects), by Italian CNR (Commessa PM.P05.012), by Italian MIUR (PRIN 2008) and by Ente CRF.

REFERENCES

(1) (a) Sanvito, S. *Nat. Phys.* **2010**, *6*, 562. (b) Sanvito, S. *Nature* **2010**, *467*, 664. (c) Rocha, A. R.; García-Suárez, V. M.; Bailey, S. W.; Lambert, C. J.; Ferrer, J.; Sanvito, S. *Nat. Mater.* **2005**, *4*, 335.

(2) Gatteschi, D.; Cornia, A.; Mannini, M.; Sessoli, R. *Inorg. Chem.* **2009**, *48*, 3408.

(3) (a) Joachim, C.; Gimzewski, J. K.; Aviram, A. *Nature* **2000**, *408*, 541. (b) Bogani, L.; Wernsdorfer, W. *Nat. Mater.* **2008**, *7*, 179. (c) Misiorny, M.; Weymann, I.; Barnas, J. *Europhys. Lett.* **2010**, *89*, 18003.

(4) (a) Mannini, M.; Sainctavit, Ph.; Sessoli, R.; Cartier dit Moulin, C.; Pineider, F.; Arrio, M.-A.; Cornia, A.; Gatteschi, D. *Chem.—Eur. J.* **2008**, *14*, 7530.(b) Saywell, A.; Magnano, G.; Satterley, C. J.; Perdigão, L. M. A.; Britton, A. J.; Taleb, N.; del Carmen Giménez-López, M.; Champness, N. R.; O'Shea, J. N.; Beton, P. H. *Nat. Commun.* **2010**, *1*:75 doi: 10.1038/ncomms1075.

(5) (a) Mannini, M.; Pineider, F.; Sainctavit, Ph.; Danieli, C.; Otero, E.; Sciancalepore, C.; Talarico, A. M.; Arrio, M.-A.; Cornia, A.; Gatteschi, D.; Sessoli, R. *Nat. Mater.* **2009**, *8*, 194. (b) Mannini, M.; Pineider, F.; Danieli, C.; Totti, F.; Sorace, L.; Sainctavit, Ph.; Arrio, M.-A.; Otero, E.; Joly, L.; Cesar, J. C.; Cornia, A.; Sessoli, R. *Nature* **2010**, *468*, 417.

(6) (a) Coronado, E.; Giménez-López, M. C.; Korzeniak, T.; Levchenko, G.; Romero, F. M.; Segura, A.; García-Baonza, V.; Cezar, J. C.; de Groot, F. M. F.; Milner, A.; Paz-Pasternak, M. *J. Am. Chem. Soc.* **2008**, *130*, 15519. (b) Prinz, M.; Kuepper, K.; Taubitz, C.; Raekers, M.; Khanra, S.; Biswas, B.; Weyhermüller, T.; Uhlarz, M.; Wosnitza, J.; Schnack, J.; Postnikov, A. V.; Schröder, C.; George, S. J.; Neumann, M.; Chaudhuri, P. *Inorg. Chem.* **2010**, *49*, 2093. (c) Khanra, S.; Kuepper, K.; Weyhermuller, T.; Prinz, M.; Raekers, M.; Voget, S.; Postnikov, A. V.; de Groot, F. M. F.; George, S. J.; Coldea, M.; Neumann, M.; Chaudhuri, P. *Inorg. Chem.* **2008**, *47*, 4605. (d) Lorusso, G.; Corradini, V.; Candini, A.; Ghirri, A.; Biagi, R.; del Pennino, U.; Carretta, S.; Garlatti, E.; Santini, P.; Amoretti, G.; Timco, G.; Pritchard, R. G.; Winpenny, R. E. P.; Affronte, M. *Phys. Rev. B* **2010**, *82*, 144420. (e) Poneti, G.; Mannini, M.; Sorace, L.; Sainctavit, Ph.; Arrio, M. A.; Otero, E.; Cezar, J. C.; Dei, A. *Angew. Chem., Int. Ed.* **2010**, *49*, 1954.

(7) (a) Wende, H.; Bernien, M.; Luo, J.; Sorg, C.; Ponpandian, N.; Kurde, J.; Miguel, J.; Piantek, M.; Xu, X.; Eckhold, Ph.; Kuch, W.; Baberschke, K.; Panchmatia, P. M.; Sanyal, B.; Oppeneer, P. M.; Eriksson, O. *Nat. Mater.* **2007**, *6*, 516. (b) Gambardella, P.; Stepanow, S.; Dmitriev, A.; Honolka, J.; de Groot, F. M. F.; Lingenfelder, M.; Gupta, S. S.; Sarma, D. D.; Bencok, P.; Stanescu, S.; Clair, S.; Pons, S.; Lin, N.; Seitsonen, A. P.; Brune, H.; Barth, J. V.; Kern, K. *Nat. Mater.* **2009**, *8*, 189. (c) Stepanow, S.; Honolka, J.; Gambardella, P.; Vitali, L.; Abdurakhmanova, N.; Tseng, T.-C.; Rauschenbach, S.; Tait, S. L.; Sessi, V.; Klyatskaya, S.; Ruben, M.; Kern, K. *J. Am. Chem. Soc.* **2010**, *132*, 11900. (d) Corradini, V.; Moro, F.; Biagi, R.; De Renzi, V.; del Pennino, U.; Bellini, V.; Carretta, S.; Santini, P.; Milway, V. A.; Timco, G.; Winpenny, R. E. P.; Affronte, M. *Phys. Rev. B* **2009**, *79*, 144419.

(8) (a) Ishikawa, N.; Sugita, M.; Ishikawa, T.; Koshihara, S.; Kaizu, Y. *J. Am. Chem. Soc.* **2003**, *125*, 8694. (b) Branzoli, F.; Filibian, M.; Carretta, P.; Klyatskaya, S.; Ruben, M. *Phys. Rev. B* **2009**, *79*, 220404(R). (c) Branzoli, F.; Carretta, P.; Filibian, M.; Zoppellaro, G.; Graf, M. J.; Galan-Mascaros, J. R.; Fuhr, O.; Brink, S.; Ruben, M. *J. Am. Chem. Soc.* **2009**, *131*, 4387.

(9) (a) Gregoli, L.; Danieli, C.; Barra, A.-L.; Neugebauer, P.; Pellegrino, G.; Poneti, G.; Sessoli, R.; Cornia, A. *Chem.—Eur. J.* **2009**, *15*, 6456. (b) Accorsi, S.; Barra, A.-L.; Caneschi, A.; Chastanet, G.; Cornia, A.; Fabretti, A. C.; Gatteschi, D.; Mortalò, C.; Olivieri, E.; Parenti, F.; Rosa, P.; Sessoli, R.; Sorace, L.; Wernsdorfer, W.; Zobbi, L. *J. Am. Chem. Soc.* **2006**, *128*, 4742. (c) Barra, A.-L.; Bianchi, F.; Caneschi, A.; Cornia, A.; Gatteschi, D.; Gorini, L.; Gregoli, L.; Maffini, M.; Parenti, F.; Sessoli, R.; Sorace, L.; Talarico, A. M. *Eur. J. Inorg. Chem.* **2007**, 4145.

(10) Mannini, M.; Pineider, F.; Sainctavit, Ph.; Joly, L.; Fraile-Rodrìguez, A.; Arrio, M.-A.; Cartier dit Moulin, Ch.; Wernsdorfer, W.; Cornia, A.; Gatteschi, D.; Sessoli, R. *Adv. Mater.* **2009**, *21*, 167.

(11) Tancini, E.; Rodriguez-Douton, M.-J.; Sorace, L.; Barra, A.-L.; Sessoli, R.; Cornia, A. *Chem.—Eur. J.* **2010**, *16*, 10482.

(12) (a) Wu, C.-H. S.; Rossman, G. R.; Gray, H. B.; Hammond, G. S.; Schugar, H. J. *Inorg. Chem.* **1972**, *11*, 990. (b) Herwig, W.; Zeiss, H. H. *J. Org. Chem.* **1958**, *23*, 1404.(c) Jeffery, J. H.; Bassett, J.; Mendham, J.; Denney, R. C. *Vogel Analisi Chimica Quantitativa*; Casa Editrice Ambrosiana: Milano, Italy, 1995; p 378.

(13) (a) Altomare, A.; Cascarano, G.; Giacovazzo, C.; Guagliardi, A. *J. Appl. Crystallogr.* **1993**, *26*, 343. (b) Sheldrick, G. M. *Acta Crystallogr.* **2008**, *A64*, 112. (c) Farrugia, L. J. *J. Appl. Crystallogr.* **1999**, *32*, 837.(d) Fleischer, H.; Schollmeyer, D. *Acta Crystallogr., Sect. E (Struct. Rep. Online)* **2001**, *57*, o330 (QIBJOA entry of CCDC). (e) Jacobsen, C. J. H.; Pedersen, E.; Villadsen, J.; Weihe, H. *Inorg. Chem.* **1993**, *32*, 1216.

(14) Pineider, F.; Mannini, M.; Danieli, C.; Armelao, L.; Piras, F. M.; Magnani, A.; Cornia, A.; Sessoli, R. *J. Mater. Chem.* **2010**, *20*, 187.

(15) (a) Goulon, J.; Brookes, N. B.; Gauthier, C.; Goedkoop, J. B.; Goulon-Ginet, C.; Rogalev, M. *Phys. B* **1995**, *208/209*, 199. (b) Englisch, U.; Rossner, H.; Maletta, H.; Bahrdt, J.; Sasaki, S.; Senf, F.; Sawhney, K. J. S.; Gudat, W. *Nucl. Instrum. Meth. A* **2001**, *467−468*, 541. (c) Flechsig, U.; Nolting, F.; Fraile Rodriguez, A.; Krempasky, J.; Quitmann, C.; Schmidt, T.; Spielmann, S.; Zimoch, D. *AIP Conf. Proc* **2010**, *1234*, 319. (d) Nakajima, R.; Stohr, J.; Idzerda, Y. U. *Phys. Rev. B* **1999**, *59*, 6421.(e) Sessoli, R.; Mannini, M.; Pineider, F.; Cornia, A.; Sainctavit, Ph. In *Magnetism and Synchrotron Radiation*; Beaurepaire, E., Bulou, H., Scheurer, F., Kappler, J. P., Eds.; Spinger-Verlag: Berlin, Germany, 2010; Springer Proceedings in Physics, Vol. 133, p 279.

(16) Crystal structure data for **3**: chemical formula $C_{96}H_{168}O_{20}S_2Fe_3Cr$, M_r = 1925.97, crystal system monoclinic, space group $C2/c$ (No. 15), a = 27.4032(15) Å, b = 20.8832(13) Å, c = 18.9981(12) Å, β = 97.929(2)°, V = 10768.0(11) Å^3, Z = 4, T = 120(2) K, λ = 0.71073 Å, $F(000)$ = 4152, D_{calcd} = 1.188 g cm^{-3}, μ = 0.593 mm^{-1}, $2\theta_{max}$ = 55.1°, 54658/12377 reflections collected/unique (R_{int} = 0.0334), final R indices $R1$ = 0.0651 ($I > 2\sigma(I)$), $wR2$ = 0.1988 (all data), GoF = 1.023, largest diff. peak and hole 0.915/−0.902 eÅ^{-3}. CCDC 793297 contains the supplementary crystallographic data for this paper. These data can be obtained free of charge from The Cambridge Crystallographic Data Centre via www.ccdc.cam.ac.uk/data_request/cif.

(17) Shannon, R. D.; Prewitt, C. T. *Acta Crystallogr., Sect. B* **1970**, *26*, 1046.

(18) Barra, A.-L.; Brunel, L. C.; Gatteschi, D.; Pardi, L.; Sessoli, R. *Acc. Chem. Res.* **1998**, *31*, 460.

(19) (a) Brice-Profeta, S.; Arrio, M.-A.; Tronc, E.; Menguy, N.; Letard, I.; Cartier dit Moulin, C.; Noguès, M.; Chanéac, C.; Jolivet, J.-P.; Sainctavit, Ph. *J. Magn. Magn. Mater.* **2005**, *288*, 354. (b) Carvallo, C.; Sainctavit, Ph.; Arrio, M.-A.; Menguy, N.; Wang, Y.; Ona-Nguema, G.; Brice-Profeta, S. *Am. Mineral.* **2008**, *93*, 880.

(20) Carlin, R. L. *Magnetochemistry*; Springer-Verlag: Berlin, Germany, 1986.